

A Novel Third-Order Leap-Frog Active Filter

DOI 10.7305/automatika.54-2.308
UDK 621.372.542.011.732.2.011.75
IFAC 2.3; 1.1.8

Original scientific paper

This paper presents the realization of third-order low-pass active-RC filters using a new Leap-Frog (LF) topology. New structure is a simplified LF structure with the elements calculated directly from the transfer function coefficients. Several versions of the circuits are presented and compared. The comparison to other common third-order filter sections is done, as well. The new LF filter has the reduced number of components, reduced complexity and straightforward design procedure compared to classical filters. As an illustration of the efficiency of the proposed new LF filter, the sensitivity analysis using Schoeffler sensitivity measure as well as output thermal noise analysis was performed on examples with Butterworth and Chebyshev 0.5dB pass-band ripple transfer functions. Using PSpice with a TL081 opamp model, the filter performance is simulated and the results compared and verified by measurements on a discrete-component breadboard filter. All equations needed for the step-by-step design are given.

Key words: Leap-Frog filters, Third-Order filter sections, Low-Sensitivity and low-noise filters, Active-RC filters

Novi aktivni leap-frog filtar trećeg reda. U radu je predstavljena realizacija nisko-propusnog aktivnog-RC filtra trećeg reda koji upotrebljava novu "leap-frog" (LF) topologiju. Nova struktura je pojednostavljena LF struktura s elementima koji se računaju direktno iz koeficijenata prijenosne funkcije. Nekoliko inačica krugova je prikazano i obavljena je usporedba. Napravljena je usporedba također i s drugim uobičajenim filtarskim sekcijama trećeg reda. Novi LF filtar ima smanjeni broj komponenata, smanjenu kompleksnost i jednostavniji postupak projektiranja u usporedbi s klasičnim filtrima. Za ilustraciju učinkovitosti predstavljenog novog LF filtra, provedena je analiza osjetljivosti pomoću Schoefflerove mjere osjetljivosti i analiza termičkog šuma na izlazu na primjerima s prijenosnim funkcijama po Butterworthu i Chebyshevu s valovitošću u području propuštanja od 0.5 dB. Pomoću PSpice-a s modelom pojačala TL081, filtarska svojstva su simulirana, uspoređena i potvrđena mjerenjima na filtrima realiziranim pomoću diskretnih elemenata na štampanoj pločici. U radu su dane sve potrebne jednadžbe u postupku projektiranja korak po korak.

Ključne riječi: leap-frog filtri, filtarske sekcije trećeg reda, niskoosjetljivi i niskošumni filtri, aktivni RC filtri

1 INTRODUCTION

In each modern mixed analog and digital signal processing device there is an 'analog front end', which, among other circuits, most frequently includes continuous-time selective filters. Continuous time filters are unavoidable as antialiasing devices for sampled data systems, but they are used for other purposes, as well. In some applications they have advantages over discrete-time filters because they do not produce sampling noise, consume less power, and finally are much simpler. Important representatives of continuous-time analog filters are active filters, either as a discrete component circuit, or realized on a chip.

However, active-RC filters very often have a disadvantage in their *high sensitivities* to component tolerances of the circuit. Reduction of sensitivities in active filters is

always a good motivation for the proposal of a new low-sensitive circuit. The sensitivity problem becomes more pronounced in the design of high-order, highly-selective filters which inevitably include large transfer function pole-Q factors.

Any low-pass filter transfer function can be realized using only one opamp and an RC network of any order [1]. However, this solution is often impractical because of high sensitivities and tuning difficulties. The problem increases with increasing pole-Q factors and in the most cases we prefer to use cascaded design which is also the simplest filter structure for building high-order filters [2].

Since it was not considered very much in the past, in this paper we try to emphasize the importance of *the third-order building blocks*. To design high-order active-

RC filters we use various first- and second-order single- or multiple-amplifier filter sections. If the filter order is even, only second-order filter building blocks are required. If the filter order is odd, then we add one first-order (single-pole) filter section. Sometimes it is more practical to combine that section with some second-order section within the filter circuit to obtain a new and compact third-order building block. It is then expected that the new third-order section possess smaller circuit complexity and reduced sensitivities compared to a cascade of first- and second-order sections. Therefore, instead of a cascade of second- and first-order filter sections, we can realize a high-order filter as a cascade of third- and second-order section, and get the reduction of overall filter sensitivities.

Some authors proposed filter realization procedures using only third-order sections in order to yield a reduction of the sensitivities of the overall filter, the reduction in number of operational amplifiers and, consequently, reduced power consumption and noise [3]. In these solutions the emphasis is on approximations of filter transfer function of any order (both even and odd), by cascading more than one third-order building block. Same authors [3] also introduced approximation techniques suitable for realization of high-order filters by cascading third-order filter sections and, if necessary, second-order sections. The main feature of this class is the introduction of a multiple real pole, in order to realize RC-active filters by cascading multiple third-order sections.

In this paper, we present a new topology of third-order active-RC filter, which has low sensitivity to component tolerances, low noise and reduced complexity. The proposed topology is based on leap-frog (LF) structure. The design procedure of the proposed circuit is simple, because the element values are calculated directly from the transfer function coefficients. The early version of the new LF filter was preliminary presented in [4].

In this paper we also present several new variations of the third-order LF filter topology. We compare them to other common third-order single- and multiple-amplifier filter blocks suitable for medium- and high-pole Q realizations. (The classification of circuits regarding low, medium, and high pole-Q factors is given in [5].) We use the sensitivities to component variations of those circuits as the most important comparison criteria, but output noise, power consumption and complexity are also taken into consideration. Multi-parametric Schoeffler sensitivity measure programmed in Matlab to investigate sensitivity of various realizations of Butterworth and Chebyshev filters of third-order is used. Detailed description of Matlab code for Schoeffler sensitivity is given in [6]. We also use the Cadence PSpice 16 program [7] to analyze the output noise with real opamp model.

In Section 2 five different variations of the new third-order LF filter are presented. Optimization of dynamic range of the new LF filter is performed numerically using Matlab Optimization Toolbox [8]. In Section 3 new LF filter structure is compared to four commonly used third-order filter sections. Section 4 presents measurement results, and Section 5 concludes this paper.

2 NEW LEAP-FROG FILTERS

As mentioned above, a third-order building block can play a very important role in the cascaded design of high-order low-pass (LP) and high-pass (HP) filters. Therefore in this section we present several new leap-frog filters suitable for realization of low- and high-pole Q factors.

2.1 New leap-frog filter (NLF)

Consider the third-order voltage transfer function of an allpole low-pass filter given in terms of the polynomial coefficients a_i ($i = 0, 1, 2$)

$$H(s) = \frac{V_{out}(s)}{V_{in}(s)} = \frac{k \cdot a_0}{s^3 + a_2 s^2 + a_1 s + a_0}, \quad (1)$$

and in factored form consider the negative-real pole γ and the complex-conjugate pole pair given in terms of the pole frequency ω_p and the pole Q, q_p ,

$$H(s) = \frac{V_{out}(s)}{V_{in}(s)} = \frac{k \cdot \gamma \omega_p^2}{(s + \gamma) \left[s^2 + \frac{\omega_p}{q_p} s + \omega_p^2 \right]}. \quad (2)$$

Note that k represents the dc-gain. The relationships between the transfer function coefficients a_i ($i = 0, 1, 2$) and pole parameters γ , ω_p and q_p are given by:

$$a_0 = \gamma \omega_p^2; \quad a_1 = \omega_p^2 + \frac{\gamma \omega_p}{q_p}; \quad a_2 = \frac{\omega_p}{q_p} + \gamma. \quad (3)$$

Third-order transfer function in (1) can be realized by the new LF third-order filter section shown in Fig. 1. It is apparent that this is a variation of well-known leap-frog topology. Since the feedback signals are fed to the positive inputs of opamps, there is no need for inverting amplifiers and the circuit has reduced number of opamps compared to the ordinary LF filter.

Transfer function coefficients a_i ($i = 0, 1, 2$), and the gain k for the section in Fig. 1 are given by

$$\begin{aligned} a_0 &= \alpha \cdot \omega_1 \cdot \omega_2 \cdot \omega_3; \\ a_1 &= (1 + \alpha) \cdot \omega_2 \omega_3 + \omega_1 \omega_2; \\ a_2 &= (1 + \alpha) \cdot \omega_3 + \omega_2; \\ k &= -1/\alpha, \end{aligned} \quad (4)$$

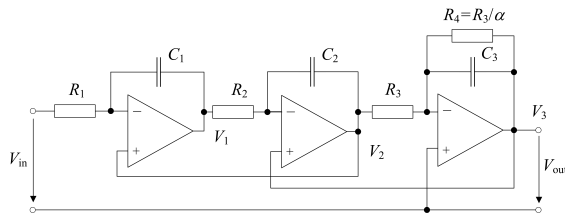


Fig. 1. New third-order low-pass LF filter

where ω_i are reciprocals of the RC-products, defined by:

$$\omega_i = (R_i C_i)^{-1} \quad (i = 1, 2, 3), \quad (5)$$

and the parameter $\alpha = R_3/R_4$. It is obvious that if $\alpha = 0$, the resistance R_4 becomes infinite, and from (4) $a_0 = 0$, meaning that the real pole of the transfer function is actually a pole at the origin. In order to realize negative real pole, α must always be non-zero and $R_4 < \infty$. The parameters ω_i can be obtained by solving the equations (4). We can start with finding ω_3 first, which gives simpler calculation. For convenience we denote

$$(1 + \alpha)\omega_3 = x, \quad (6)$$

and obtain the following set of equations:

$$\begin{aligned} x^3 - a_2 x^2 + a_1 x - a_0 \frac{1+\alpha}{\alpha} &= 0 \Rightarrow \omega_3 = \frac{x}{1+\alpha}; \\ \omega_2 = a_2 - (1 + \alpha)\omega_3; \quad \omega_1 &= \frac{a_0}{\alpha \cdot \omega_2 \cdot \omega_3}. \end{aligned} \quad (7)$$

Note that α is an arbitrary positive nonzero constant, which determines the pass-band gain k , as well. Finally, we have to choose C_1, C_2 and C_3 , and from known ω_i resistors R_i ($i = 1, 2, 3$) readily follow using:

$$R_i = (\omega_i C_i)^{-1} \quad (i = 1, 2, 3). \quad (8)$$

Examples: As an illustration of the design procedure above, consider two examples of third-order LP filter transfer functions with the cut-off frequency 1kHz: (i) Butterworth, and (ii) Chebyshev with the pass-band ripple $A_{max} = 0.5$ dB. A Butterworth filter has 'maximally flat' amplitude response and corresponds to the limit case of no ripple in the filter pass-band. Compared to a Chebyshev filter of equal order, it has lower pole Qs.

It is well known that the higher the ripple, the higher are the pole Qs, and consequently the sensitivities to component tolerances and noise, as well. Since we investigate both properties, these two approximation examples are suitable because they provide two different pole Q-factors: i.e. $q_p = 1$ (low-Q example for the Butterworth filter), and $q_p = 1.70619$ (somewhat higher pole-Q value in the example for the Chebyshev filter). Coefficients a_i ($i = 0, 1, 2$)

Table 1. Third-order Butterworth and Chebyshev transfer-function parameters with 1kHz cut-off frequency

Coefficients and pole parameters					
Parameter		Butterworth		Chebyshev 0.5 dB	
a_0	γ	$2.4805 \cdot 10^{11}$	$6.2832 \cdot 10^3$	$1.7753 \cdot 10^{11}$	$3.3936 \cdot 10^3$
a_1	ω_p	$7.8957 \cdot 10^7$	$6.2832 \cdot 10^3$	$6.0595 \cdot 10^{11}$	$6.7158 \cdot 10^3$
a_2	q_p	$1.2566 \cdot 10^4$	1.0	$7.8723 \cdot 10^3$	1.70619

Table 2. Component values of Butterworth and Chebyshev examples of the circuit in Fig. 1

Component values (resistors in kΩ, capacitors in nF)					
Component		Butterworth		Chebyshev 0.5 dB	
R_1	C_1	5.6055	10	2.1828	10
R_2	C_2	34.879	10	86.692	10
R_3	C_3	20.620	10	29.767	10
R_4		20.620		29.767	10

and the corresponding pole parameters ω_p, q_p and γ , and dc-gain k for these examples are calculated using Matlab and are given in Table 1. Note that we realize pass-band gain with $k = 1$, therefore we choose $\alpha = 1$.

Starting from parameters in Table 1 and using design equations from (6) to (8), we choose $C_1 = C_2 = C_3 = C_{TOT}/3 = 10$ nF (i.e. we have total capacitance $C_{TOT} = 30$ nF) and obtain element values of Butterworth and Chebyshev filters presented in Table 2.

Both filters are realized by the circuit in Fig. 1 and their transfer function magnitudes $\alpha(\omega) = 20 \log |H(j\omega)|$ [dB] are shown in Fig. 6(a)–(b) in Section 2.6.

2.2 New leap-frog filter–Variation form 1 (VAR 1)

Alternative way to realize transfer function pole on the negative real-axis of the s -plane is to introduce a negative feedback from the output to the input of a circuit from Fig. 1 as shown in Fig. 2 (this requires *four* opamps).

Transfer function coefficients a_i ($i = 0, 1, 2$), and the gain k for the section in Fig. 2 are given by

$$\begin{aligned} a_0 &= \alpha \cdot (1 + \beta) \cdot \omega_1 \cdot \omega_2 \cdot \omega_3; \\ a_1 &= \omega_2 \omega_3 + \omega_1 \omega_2; \\ a_2 &= \omega_2 + \omega_3; \\ k &= -\beta / [\alpha(1 + \beta)], \end{aligned} \quad (9)$$

where ω_i are defined by (5) above and for this case $\alpha = R_5/(R_4 + R_5)$. Parameters ω_i can be calculated by solving the following equations:

$$\begin{aligned} \omega_3^3 - a_2 \omega_3^2 + a_1 \omega_3 - \frac{a_0}{\alpha(1+\beta)} &= 0 \Rightarrow \omega_3; \\ \omega_2 = a_2 - \omega_3; \\ \omega_1 &= \frac{a_0}{\alpha(1+\beta)\omega_2\omega_3}. \end{aligned} \quad (10)$$

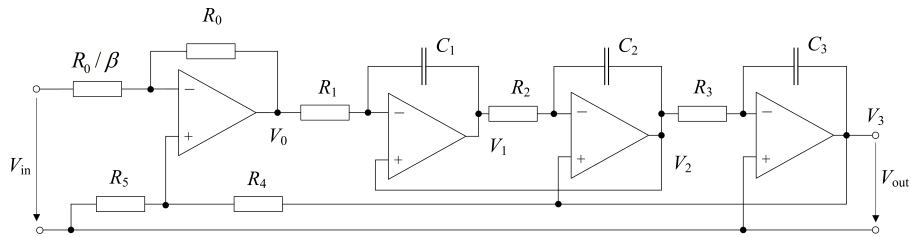


Fig. 2. Third-order low-pass LF filter VAR 1

Table 3. Component values of Butterworth and Chebyshev examples of the circuit in Fig. 2

Component values (resistors in kΩ, capacitors in nF)					
Component		Butterworth		Chebyshev 0.5 dB	
R_1	C_1	15.915	10	8.7272	10
R_2	C_2	15.915	10	25.405	10
R_3	C_3	15.915	10	25.405	10

In the design example we choose $\alpha = 0.5$, $\beta = 1$, $C_1 = C_2 = C_3 = 10$ nF, i.e. the same $C_{TOT} = 30$ nF as in the design of the circuit (in Fig. 1) in Section 2.1. For the purpose of comparing the noise performance of different filter circuits we assume the same total capacitance. From calculated ω_i , resistors R_i ($i = 1, 2, 3$) readily follow from (8). Finally, we choose $R_0 = R_4 = 10$ kΩ and calculate $R_5 = R_4(1/\alpha - 1) = 10$ kΩ. We obtain element values presented in Table 3.

2.3 New leap-frog filter–Variation form 2 with reduced amplifiers (VAR 2)

In the last design a summing amplifier can be thrown out if we feed the output signal to the negative input of the first integrator as shown in Fig. 3 (three opamps are required).

Transfer function coefficients a_i ($i = 0, 1, 2$), and the gain k for this section are given by

$$\begin{aligned} a_0 &= \alpha \cdot \omega_1 \cdot \omega_2 \cdot \omega_3; \\ a_1 &= (1 + \alpha)\omega_1\omega_2 + \omega_2\omega_3; \\ a_2 &= \omega_2 + \omega_3; \\ k &= 1/\alpha, \end{aligned} \tag{11}$$

where ω_i are defined by (5). Parameters ω_i can be obtained by solving the following equations:

$$\begin{aligned} \omega_3^3 - a_2\omega_3^2 + a_1\omega_3 - \frac{a_0(1+\alpha)}{\alpha} &= 0 \Rightarrow \omega_3; \\ \omega_2 &= a_2 - \omega_3; \\ \omega_1 &= \frac{a_0}{\alpha\omega_2\omega_3}. \end{aligned} \tag{12}$$

In the design example we choose $\alpha = 1$, $C_1 = C_2 = C_3 = 10$ nF, and from calculated ω_i , resistors R_i ($i = 1, 2, 3$) readily follow from (8). The resulting element values are given in Table 4.

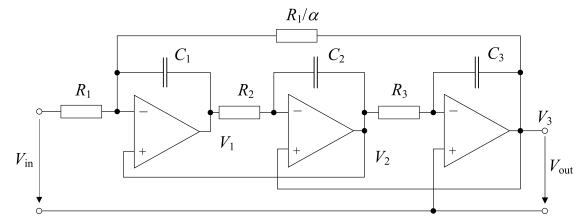


Fig. 3. Third-order LF filter VAR 2

Table 4. Component values of Butterworth and Chebyshev examples of the circuit in Fig. 3

Component values (resistors in kΩ, capacitors in nF)					
Component		Butterworth		Chebyshev 0.5 dB	
R_1	C_1	11.211	10	4.3656	10
R_2	C_2	34.879	10	86.629	10
R_3	C_3	10.310	10	14.884	10

2.4 New leap-frog filter–Weighted feedback solution with reduced amplifiers (VAR 3)

Sometimes there is a need for reducing the amount of feedback signals in the LF circuit as shown in Fig. 4. Feedback signals are reduced by voltage dividers consisting of additional resistors R_0 and R_{0i} ($i = 1, 2$), and by that the feedback is weaker.

Transfer function coefficients a_i ($i = 0, 1, 2$), and the gain k for the section in Fig. 4 are given by

$$\begin{aligned} a_0 &= \alpha \cdot \omega_1 \cdot \omega_2 \cdot \omega_3; \\ a_1 &= \beta_1(1 + \alpha)\omega_1\omega_2 + \beta_2\omega_2\omega_3; \\ a_2 &= \beta_1\omega_2 + \beta_2\omega_3; \\ k &= 1/\alpha, \end{aligned} \tag{13}$$

where $\beta_1 = R_0/(R_0 + R_{01})$, $\beta_2 = R_0/(R_0 + R_{02})$, and ω_i are defined by (5) above. Parameters ω_i can be obtained by solving the following equations:

$$\begin{aligned} \omega_3^3 - \frac{a_2}{\beta_2}\omega_3^2 + \frac{a_1\beta_1}{\beta_2^2}\omega_3 - \frac{a_0\beta_1^2(1+\alpha)}{\alpha\beta_2^2} &= 0 \Rightarrow \omega_3; \\ \omega_2 &= \frac{a_2 - \beta_2\omega_3}{\beta_1}; \\ \omega_1 &= \frac{a_0}{\alpha\omega_2\omega_3}. \end{aligned} \tag{14}$$

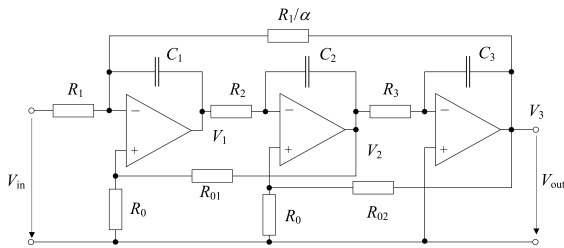


Fig. 4. Third-order LF filter VAR 3

Table 5. Component values of Butterworth and Chebyshev examples of the circuit in Fig. 4

Component values (resistors in kΩ, capacitors in nF)					
Component		Butterworth		Chebyshev 0.5 dB	
R_1	C_1	52.451	10	31.627	10
R_2	C_2	13.712	10	9.7221	10
R_3	C_3	56.055	10	18.319	10

In the design, the values of β_1 , β_2 and α can be used for optimization of dynamic range. In this example we choose $\alpha = 1$, $\beta_1 = \beta_2 = 0.5$, $C_1 = C_2 = C_3 = 10$ nF, and from calculated ω_i resistors R_i ($i = 1, 2, 3$) readily follow from (8). Finally, we choose R_0 and calculate feedback resistors $R_{0i} = R_0(1/\beta_i - 1)$ ($i = 1, 2$). Choosing $R_0 = 10$ kΩ we have obtained $R_{01} = R_{02} = 10$ kΩ, and the remaining element values are presented in Table 5.

2.5 Dynamic range optimization of the 'new LF filter'

Consider our new LF filter in Fig. 1 with additional voltage attenuators (as in Fig. 4) for reduction of the amount of feedback signals needed for dynamic range optimization. Filter circuit with optimization capability is shown in Fig. 5, where $\beta_1 = R_0/(R_0 + R_{01})$, $\beta_2 = R_0/(R_0 + R_{02})$, and the parameter $\alpha = R_3/R_4$. In the sequel β_1 , β_2 and α are used for optimization process. Preliminary results on dynamic range optimization are given in [9].

Transfer function coefficients a_i ($i = 0, 1, 2$), and the gain k for the section in Fig. 5 are given by

$$\begin{aligned}
 a_0 &= \alpha\beta_1\omega_1\omega_2\omega_3; \\
 a_1 &= (\alpha\beta_1 + \beta_2)\omega_2\omega_3 + \beta_1\omega_1\omega_2; \\
 a_2 &= (\alpha + \beta_2)\omega_3 + \beta_1\omega_2; \\
 k &= -1/(\alpha\beta_1).
 \end{aligned} \tag{15}$$

The parameters ω_i ($i = 1, 2, 3$) can be obtained by solving the following equations:

$$\begin{aligned}
 \omega_3^3 - \omega_3^2 \frac{a_2}{\alpha + \beta_2} + \omega_3 \frac{a_1}{X} - \frac{a_0}{\alpha X} &= 0, \\
 \text{where } X &= (\alpha + \beta_2/\beta_1)(\alpha + \beta_2); \\
 \omega_2 &= \frac{a_2 - (\alpha + \beta_2)\omega_3}{\beta_1}; \quad \omega_1 = \frac{a_0}{\beta_1\alpha\omega_2\omega_3}.
 \end{aligned} \tag{16}$$

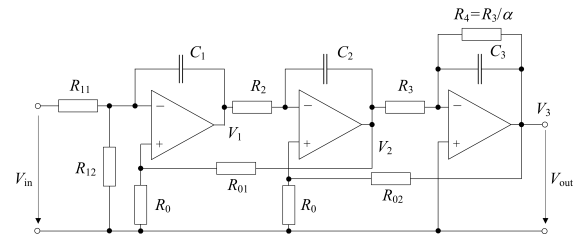


Fig. 5. Third-order new LF filter with additional resistors for dynamic range optimization

In the first example we choose $C_1 = C_2 = C_3 = 10$ nF, and $\alpha = 1$, $\beta_1 = \beta_2 = 1$, which provides unity d.c. gain, i.e. $k = 1/(\alpha\beta_1) = 1$. Note that in the case when $\beta_1 = \beta_2 = 1$, design equations (16) simplify into (7), and the filter circuit in Fig. 5 simplifies into the circuit in Fig. 1.

Voltage transfer functions of every opamp output to the input are defined by:

$$H_i(s) = \frac{V_i(s)}{V_{in}(s)} = \frac{N_i(s)}{D(s)}; \quad (i = 1, 2, 3), \tag{17}$$

with numerators given by:

$$\begin{aligned}
 N_1(s) &= -\omega_1 [s^2 + (\beta_2 + \alpha)\omega_3s + \omega_2\omega_3\beta_2]; \\
 N_2(s) &= (s + \alpha\omega_3)\omega_1\omega_2; \\
 N_3(s) &= -\omega_1\omega_2\omega_3.
 \end{aligned} \tag{18}$$

Note that all transfer functions in (17) have the same denominator $D(s) = s^3 + a_2s^2 + a_1s + a_0$, with coefficients a_i ($i = 1, 2, 3$) defined by (15).

The amplitude-frequency characteristics of the transfer functions in (17), i.e. $A_i(\omega)[dB] = 20 \log |H_i(j\omega)|$ ($i = 1, 2, 3$), were simulated using Cadence PSpice 16 with TL081/TI opamp model and are shown in Fig. 6(a) and (b) for Butterworth and Chebyshev examples, respectively. As can be seen in Fig. 6(a) and (b) the magnitudes of inner opamp outputs have *different* maximal values than 0dB (all maximums are designated). Maximum of $A_3(\omega)$ is at 0dB. Note also that filter circuit behaves well up to 500kHz where it has attenuation of 150dB.

One criterion that is useful to guarantee maximum dynamic range is to specify that the maximum signal level at any node within the circuit should at no time exceed the signal level at the input or output. On the other hand if some of the nodes have much lower signal level than those at the other nodes, it also deteriorates the dynamic properties of the filter. Thus, for input signal equal to 1V the largest signal within the circuit should everywhere in the circuit (i.e. at every opamp output) be equal to 1V, or in

other words, the maximum gain of magnitude characteristic must be equal to 0dB.

A simple way of signal level scaling within a circuit is to scale the corresponding nodes in the equivalent signal-flow graph (SFG) as shown in [10]. In our case of single-ended circuit this approach is not possible because the feedback signals come into the positive opamp inputs (see Fig. 5). Forward transfer function and feedback function of each amplifier in the circuit are not the same as it is in standard LF circuits, and simple rules shown in [10] for dynamic range optimization are not applicable in this case. Furthermore, in the SFG method it must be known in advance by which factors to scale the nodes, whereas, in our case, scaling factors are calculated at the end of the numerical optimization. Therefore, we must perform an optimization procedure using MATLAB or some other tool. However, the method using SFG-optimization would be possible if we constructed the fully balanced circuit with differential-input-differential-output opamps.

The only way to increase dynamic range is to determine the free design parameters α , β_1 , and β_2 to obtain equal maximums of $A_i(\omega)$ [dB], using numerical optimization procedure. We used the Matlab Optimization Toolbox [8]. In optimization, we define the quantity ϵ , which represents the sum of the squares of the distances between three magnitude maximums and the arithmetical mean of those maximums defined by z . So the error of the desired "equal-maximums" will be given by:

$$\epsilon = \sum_{i=1}^3 (|H_i(j\omega)|_{\max} - z)^2; \quad z = \frac{1}{3} \sum_{i=1}^3 |H_i(j\omega)|_{\max} \tag{19}$$

Error ϵ will be used as a 'goal' (or 'cost') function in the optimization procedure and has to be minimized. Thus, the optimum design parameters α , β_1 , and β_2 are determined by searching the minimum of "equal- maximums" error in (19), i.e.:

$$\mathbf{x}_{opt} = \arg \min_x \epsilon, \tag{20}$$

where:

$$\mathbf{x} = [\alpha \quad \beta_1 \quad \beta_2]^T. \tag{21}$$

During the optimization iterations, as we approach to minimum ϵ , the mean value z in (19) is recalculated every time, which forces that all three maximums converge to the same level defined by z .

To find $|H_i(j\omega)|_{\max}$ ($i = 1, 2, 3$) in (19) we first have to find frequencies of maximums. Using first derivatives, i.e.

$$\frac{d|H_i(j\omega)|^2}{d\omega} = 0 \quad (i = 1, 2, 3), \tag{22}$$

and because $|H_i(j\omega)|^2 = H_i(\omega^2)$ with substitution $\omega^2 = x$ we obtain the following equations for the solution of (22):

$$\begin{aligned} x^3 + \frac{a_2^2 - 2a_1 + 3\alpha^2\omega_3^2}{2}x^2 + \alpha^3\omega_3^2(a_2^2 - 2a_1)x + \alpha^2\omega_3^2(a_1^2 - 2a_0a_2) - a_0^2 &= 0 & (i = 1); \\ x^4 + 2Xx^3 + (XY - Z + W)x^2 + & & \\ + 2(WY - a_0^2)x + WZ - Xa_0^2 &= 0 & (i = 2); \\ X = \omega_3^2(\alpha + \beta_2)^2 - 2\beta_2\omega_2\omega_3; \quad Y = a_2^2 - 2a_1; & & \\ Z = a_1^2 - 2a_0a_2; \quad W = \beta_2^2\omega_2^2\omega_3^2 & & \\ \omega = 0 & & (i = 3). \end{aligned} \tag{23}$$

Positive and real roots x_i yield values $\omega_{i\max} = \sqrt{x_i}$ ($i = 1, 2, 3$), that are introduced into the frequency characteristics of (17) providing the maximum values $|H_i(j\omega)|_{\max}$ for goal function ϵ defined by (19).

For searching minimum in (20) a 'Quasi-Newton line search' method was used performing the unconstrained minimization of the goal function (19) (Matlab function `fminunc` is used) [11]. Starting with vectors \mathbf{x}_{start} we obtain solutions \mathbf{x}_{opt} :

$$\mathbf{x}_{start} = \begin{bmatrix} 0.9 \\ 0.3 \\ 0.6 \end{bmatrix}, \mathbf{x}_{opt} = \begin{bmatrix} 0.87223440964 \\ 0.28818425973 \\ 0.57509193104 \end{bmatrix}, \tag{24}$$

for Butterworth, and:

$$\mathbf{x}_{start} = \begin{bmatrix} 0.5 \\ 0.3 \\ 0.3 \end{bmatrix}, \mathbf{x}_{opt} = \begin{bmatrix} 0.59086092676 \\ 0.31040131850 \\ 0.23091201839 \end{bmatrix}, \tag{25}$$

for Chebyshev functions, respectively. After 12 iterations the precision of $\epsilon \approx 10^{-13}$ was achieved,¹ which is more than sufficient for our optimization problem. All three maximums converged to z , which represents the d.c. gain of the final filter circuit. If, for convenience, we denote z in dB as $A_0 = 20 \log(z)$ we have: $A_{0Butt} = 11.9939$ dB for Butterworth and $A_{0Cheby} = 14.7318$ dB for Chebyshev filters, respectively. Depending on the choice of starting vector \mathbf{x}_{start} we can obtain different solutions for α s and β s (contained in \mathbf{x}_{opt}) and different values of equal maximums A_{0Butt} and A_{0Cheby} . It is important that α s and

¹It is important to choose good starting point \mathbf{x}_{start} which will lead to local minimum of ϵ . In our case, the minimum equal to zero provides acceptable solution, although there can be many solutions \mathbf{x}_{opt} providing cost $\epsilon = 0$.

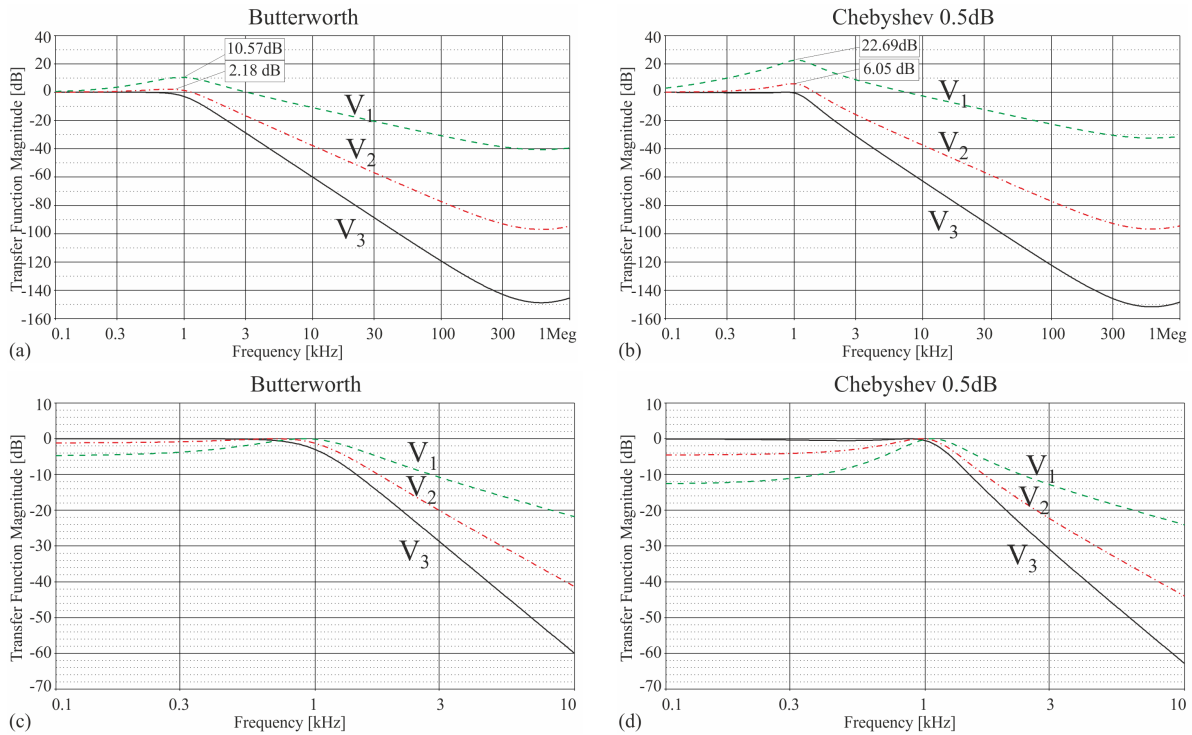


Fig. 6. PSpice magnitudes response of the new leap-frog third-order LP filters at the opamps outputs. (a)–(b) Un-optimized. (c)–(d) Optimized

β s are positive and real, and β s have to be lower than or equal to unity. There exists no rule for choosing starting vector \mathbf{x}_{start} other than 'trial-and-error'. It can also happen that due to the bad starting vector, the process does not converge to any minimum (i.e. $\epsilon > 0$).

To realize maximum 0 dB of the overall transfer function magnitude, instead obtained A_0 dB, input resistor R_1 is split into two resistors R_{11} and R_{12} and realize voltage attenuator with:

$$\mu = \frac{R_{12}}{R_{11} + R_{12}}; R_1 = \frac{R_{11}R_{12}}{R_{11} + R_{12}}, \quad (26)$$

where the value of μ readily follows from:

$$\mu = 1/k = 10^{-A_0/20} = \alpha\beta_1. \quad (27)$$

Corresponding resistors in the attenuator follow from:

$$R_{11} = R_1/\mu; R_{12} = R_1/(1 - \mu). \quad (28)$$

We also choose $R_0 = 10 \text{ k}\Omega$ and calculate feedback resistors $R_{0i} = R_0/(1/\beta_i - 1)$ ($i = 1, 2$). The component values of optimized filters are listed in Table 6, and the corresponding transfer function magnitudes of three opamp outputs are given in Fig. 6(c)–(d) for Butterworth and Chebyshev examples, respectively. In Fig. 6(c) and (d) one can clearly see the result of optimization, because all maximums are equal and at 0 dB.

Table 6. Component values of Butterworth and Chebyshev examples of the circuit in Fig. 5

Component values (resistors in k Ω , capacitors in nF)					
Component		Butterworth		Chebyshev 0.5 dB	
R_1	C_1	4.9453	10	4.6947	10
R_2	C_2	15.087	10	15.830	10
R_3	C_3	13.582	10	13.902	10
R_4	R_{01}	15.571	24.70	23.528	22.216
R_0	R_{02}	10	7.388	10	33.307
R_{11}	R_{12}	19.674	6.606	25.598	5.7490

2.6 Sensitivity and noise analysis of all new LF filter solutions

According to the classification in [5] all variants of the new LF filter in this section are suitable for high-pole Q realizations because of their inherent low sensitivities.

A multi-parametric sensitivity analysis based on Schoeffler sensitivity measure was performed on the five filter circuits having new LF topology shown in Figs. 1 to 5. If the resistor and capacitor values (in Tables 2 to 6) are assumed to be uncorrelated random variables, with zero-mean and 1% standard deviation, then the Schoeffler sensitivity approximates the variance σ_H^2 of the magnitude transfer function variations $\Delta|H(\omega)|/|H(\omega)|$. The stan-

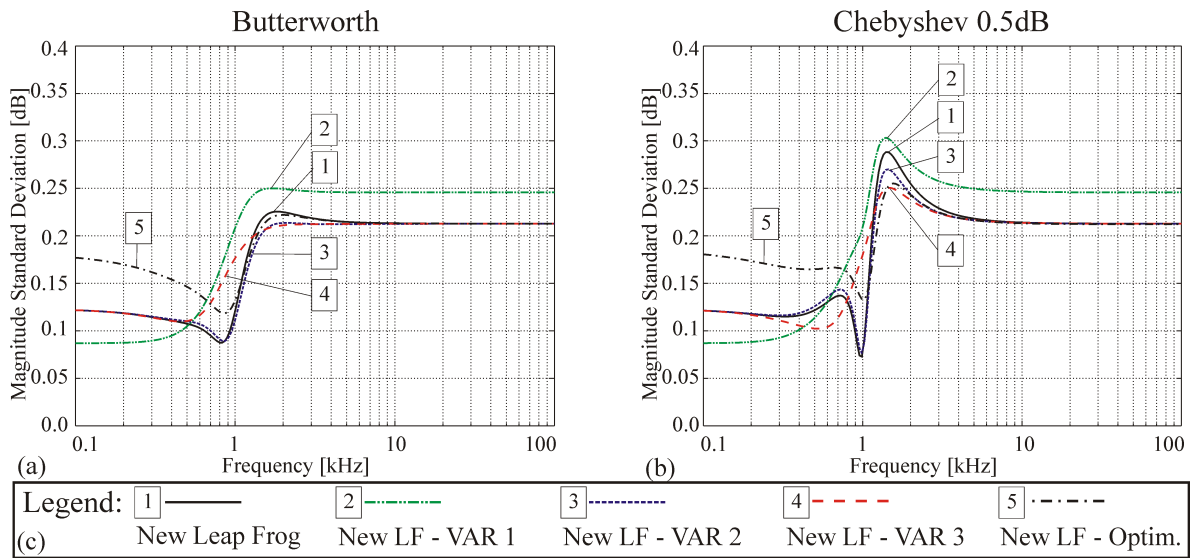


Fig. 7. Schoeffler sensitivities of new third-order leap-frog filter and its alternative solutions (Matlab simulation). (a) Butterworth. (b) Chebyshev 0.5dB. (c) Legend

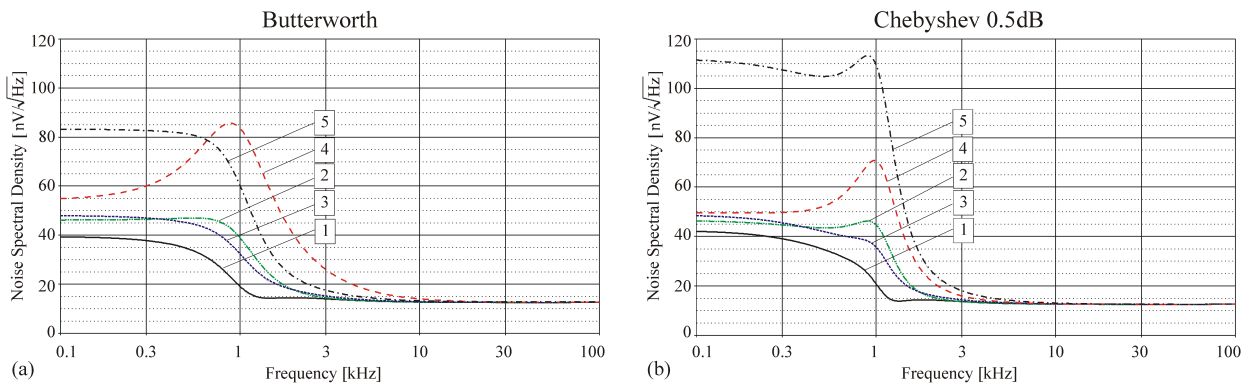


Fig. 8. PSpice output noise spectral density of new third-order leap-frog filter and its alternative solutions (legend is in Fig. 7). (a) Butterworth. (b) Chebyshev 0.5dB

dard deviation $\sigma_{\alpha}(\omega)[dB]$ of the variation of the log gain $\Delta\alpha = 8.68588\Delta|H(\omega)|/|H(\omega)|[dB]$ was calculated, with respect to all passive components, and plotted using Matlab for these circuits in Fig. 7.

There are five different plots in Fig. 7(a) and (b) for Butterworth and Chebyshev approximations, respectively. Observing Fig. 7, we can conclude that the best (lowest) sensitivity in the pass-band has the circuit no. 2, i.e. variation form 1 (VAR 1), whereas in the stop band it has worst sensitivity. All other examples have similar sensitivities at high and low frequencies except filter no. 5, i.e. new LF optimized, which possess highest sensitivity in the pass-band, but low sensitivity in the transient-band (in the vicinity of the cut-off frequency). In the transition band the best sensitivity property has the circuit no. 4, i.e. VAR

3—weighted feedback solution with reduced amplifiers.

Using the PSpice program output thermal noise spectral density of 5 filter examples in this Section was generated and shown in Fig. 8. From Fig. 8 one can conclude that the minimum noise possesses new LF filter no. 1 and the highest noise have filters no. 4 and 5, because they have additional four resistors for scaling opamps output levels.

3 COMPARISON OF NEW THIRD-ORDER LF FILTERS WITH CONVENTIONAL FILTERS

In this section we compare the most promising solution of the new third-order leap-frog filter circuit from Section 2 to several standard third-order filters. Some of these examples readily follow from [4] and [12]. The normalized circuits presented in [4] and [12] are denormalized to

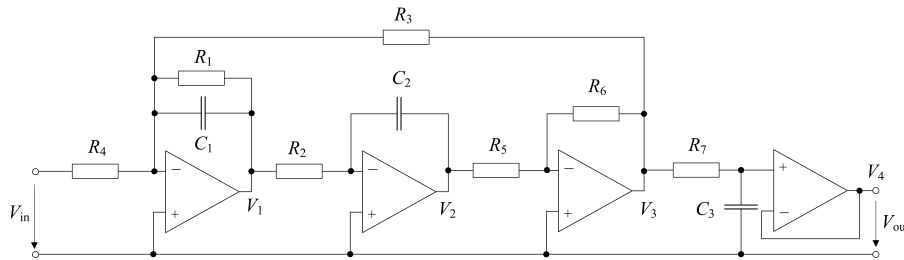


Fig. 11. Tow-thomas third-order filter

$$\begin{aligned}
 k &= \alpha\beta; a_0 = \frac{1}{R_1 R_2 R_3 C_1 C_2 C_3}; \\
 a_1 &= \frac{R_1 C_1 + (R_1 + R_2 + R_3) C_3 + (1 - \beta) C_2 (R_1 + R_2)}{R_1 R_2 R_3 C_1 C_2 C_3}; \\
 a_2 &= \frac{R_2 C_3 (R_1 C_1 + R_3 C_2) + R_1 R_3 C_3 (C_1 + C_2) + (1 - \beta) R_1 R_2 C_1 C_2}{R_1 R_2 R_3 C_1 C_2 C_3};
 \end{aligned} \tag{29}$$

where

$$\alpha = \frac{R_{12}}{R_{11} + R_{12}}; R_1 = \frac{R_{11} R_{12}}{R_{11} + R_{12}}; \beta = 1 + \frac{R_F}{R_G}. \tag{30}$$

This circuit belongs to the class of active-RC filters with single opamp and positive feedback (Sallen and Key [SAK] type). Element values of SAK filters readily follow using well-known design procedure in [2] which is optimal because it provides low-sensitivity filter circuits. To design optimum filter circuits, the *capacitive tapering* (by factor $\rho = 3$, i.e. $C_2 = C_1/\rho$; $C_3 = C_1/\rho^2$) with values $R_2 \cong R_3$ is used. Element values for both Butterworth and Chebyshev examples are given in Table 8. From R_1 we calculate $R_{11} = R_1/\alpha$ and $R_{12} = R_1/(1 - \alpha)$. We also choose $R_G = 10 \text{ k}\Omega$ and calculate $R_F = R_G(\beta - 1)$.

3.3 Tow-Thomas third-order filter

Voltage transfer functions in (1) can also be realized using a cascade of a Biquad and an RC section for realization of a real pole shown in Fig. 11. It uses the Tow-Thomas Biquad or the multi-amplifier Biquad [5].

Transfer function pole parameters, and the gain k for the circuit in Fig. 11 are given by:

$$\begin{aligned}
 k &= \frac{R_3}{R_4}; \omega_p = \frac{1}{\sqrt{R_2 R_3 C_1 C_2}}; \\
 q_p &= R_1 \sqrt{\frac{C_1}{R_2 R_3 C_2}}; \gamma = \frac{1}{R_7 C_3}.
 \end{aligned} \tag{31}$$

The circuit in Fig. 11 has proved to be advantageous for various reasons including its good dynamic-range properties, and its excellent tuning properties. To realize the third-order allpole transfer function this circuit needs *four* opamps. Element values, using the design steps in [4] for both Butterworth and Chebyshev examples, are given in Table 9.

Table 9. Component values of Butterworth and Chebyshev examples of the circuit in Fig. 11

Component values (resistors in kΩ, capacitors in nF)					
Component		Butterworth		Chebyshev 0.5 dB	
$R_{1,7}$	C_1	15.915	10	25.406	10
R_2	C_2	15.915	10	15.915	10
$R_{3,4}$	C_3	15.915	10	13.931	10
$R_{5,6}$		10		10	

Table 10. Component values of Butterworth and Chebyshev examples of the circuit in Fig. 12

Component values (resistors in kΩ, capacitors in nF)					
Component		Butterworth		Chebyshev 0.5 dB	
R_0	C_1	17.0	10	30	10
R_1	C_2	21.538	10	92.568	10
$R_{2,6}$	C_3	10	10	10	10
R_3	R_7	4.8401	48.996	6.4941	28.913

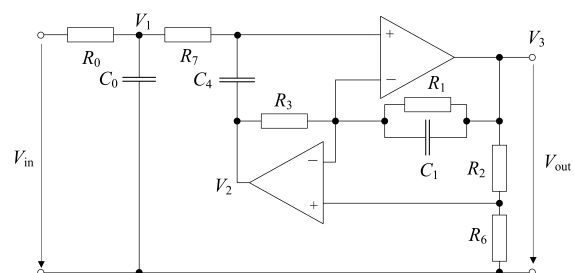


Fig. 12. GIC-based third-order filter

3.4 GIC-based third-order filter

Voltage transfer function in (1) can also be realized by a cascade of a GIC-based Biquad [5] and an RC section for realization of a real pole shown in Fig. 12 (see also [12]). Note that this circuit uses only *two* opamps. In this paper we present the design steps of the third-order GIC-based filter section. Transfer function coefficients a_i ($i = 0, 1, 2$), and the gain k for the circuit in Fig. 12 are given by:

$$\begin{aligned}
 a_0 &= \frac{\frac{R_6}{R_2}}{R_0 R_3 R_7 C_0 C_1 C_4}; \quad a_1 = \frac{(R_0 + R_7) R_3 C_4 + R_0 R_1 C_0 \frac{R_6}{R_2}}{R_0 R_1 R_3 R_7 C_0 C_1 C_4}; \\
 a_2 &= \frac{(R_0 + R_7) R_1 C_1 + R_0 R_7 C_0}{R_0 R_1 R_7 C_0 C_1}; \quad k = 1 + \frac{R_2}{R_6}.
 \end{aligned}
 \tag{32}$$

There are 9 components to be calculated from 4 conditions. Because there are 5 degrees of freedom the filter design can be performed in various ways. For the GIC filter we will choose: $R_2 = R_6 = 10 \text{ k}\Omega$ (i.e., we assume $k = 2$ and simplify the calculation because there are 3 conditions left). Furthermore, we choose $C_0 = C_1 = C_4 = 10 \text{ nF}$ and the only free parameter left is R_0 . If we define a new quantity called 'design frequency':

$$\omega_0 = 1/(R_0 C_0), \tag{33}$$

we have a new free parameter ω_0 depending on the choice of R_0 . We introduce the following notations:

$$R_1 = r_1 R_0, R_3 = r_3 R_0, R_7 = r_7 R_0, \tag{34}$$

and

$$\alpha_i = \frac{a_i}{\omega_0^{3-i}}; \quad (i = 0, 1, 2). \tag{35}$$

By application of (33)–(35) to (32), and after some calculations we obtain:

$$\begin{aligned}
 \alpha_0 &= \frac{a_0}{\omega_0^3} = \frac{1}{r_3 r_7}; \quad \alpha_1 = \frac{a_1}{\omega_0^2} = \frac{r_3 + r_3 r_7 + r_1}{r_1 r_3 r_7}; \\
 \alpha_2 &= \frac{a_2}{\omega_0} = \frac{r_1 + r_1 r_7 + r_7}{r_1 r_7}.
 \end{aligned}
 \tag{36}$$

Parameters r_1 , r_3 , and r_7 can then be calculated from the following equations:

$$\begin{aligned}
 r_1^2 (\alpha_1 - \alpha_0) - \alpha_2 r_1 + 1 &= 0 \Rightarrow r_1, \text{ i.e.,} \\
 (r_1)_{1,2} &= \frac{\alpha_2 \pm \sqrt{\alpha_2^2 - 4(\alpha_1 - \alpha_0)}}{2(\alpha_1 - \alpha_0)} = \frac{\alpha_2 \pm \sqrt{\Delta}}{2(\alpha_1 - \alpha_0)}; \\
 r_3 &= \frac{r_1(\alpha_1 - \alpha_0) - 1}{\alpha_0}; \quad r_7 = \frac{1}{r_3 \alpha_0}.
 \end{aligned}
 \tag{37}$$

It is advisable to choose a larger value for r_1 for the reason that will be explained in the sequel.

Realizability constraints: all solutions for r_1 , r_3 and r_7 in (37) must be real and positive. To calculate *real* solution for r_1 we must have discriminant under the square root $\Delta = \alpha_2^2 - 4(\alpha_1 - \alpha_0) \geq 0$; from this we calculate the following constraint on the free parameter ω_0 :

$$\omega_0 \leq \frac{4a_0}{4a_1 - a_2^2} = \omega_{0 \max}. \tag{38}$$

Furthermore, there exists always one *positive* solution for r_1 ; and if $\omega_0 > \omega_{0 \min} = a_0/a_1$ then both solutions for r_1 are positive. In the latter case, if we choose the larger

value for r_1 we ensure positive solution for r_3 . This is because the realizability constraint on the positive value of r_3 (if we have chosen larger solution for r_1) is upper bounded by the maximum frequency ω_a , which follows from:

$$-\omega_0^3 + a_2 \omega_0^2 - a_1 \omega_0 + a_0 = 0 \Rightarrow \omega_a, \tag{39}$$

and it is $\omega_a = \omega_{0 \max}$. Therefore, in the design, user can simply choose several values for ω_0 , with $\omega_{0 \min} < \omega_0 < \omega_{0 \max}$ then choose larger solution for r_1 (to obtain all component values real and positive) and select the most appropriate ω_0 until component spread is not too large.

Element values using the above design equations for both Butterworth and Chebyshev examples are in Table 10.

3.5 Sensitivity and noise analysis of the new LF filter compared to the standard filter circuits

A multi-parametric sensitivity analysis using Schoeffler measure, as above, was performed on the filter examples in Figs. 9 to 12, having element values in Tables 7 to 10 with 1% tolerances of passive elements. The standard deviation $\sigma_\alpha(\omega)$ [dB] of the transfer function magnitude, for those circuits, was plotted in Fig. 13 using Matlab. The sensitivity curves for the 'new LF' and 'optimized new LF' filters proposed in the Section 2 are also added for the comparison. Thus, there exist six different plots in Fig. 13(a) and (b) for Butterworth and Chebyshev approximations, respectively. Output thermal noise spectral densities of the same six filters were generated using PSpice and plotted in Fig. 14.

Observing Fig. 13 we can conclude that the best (lowest) sensitivity in the pass-band has the circuit no. 4, i.e. the single-amplifier Biquad. In the stop band no. 1 standard leap-frog, and no. 2 Tow-Thomas circuits show worst sensitivity. In the transition band, i.e. in the vicinity of the cut-off frequency, the lowest sensitivities have circuits no. 5 and 6, i.e. new LF circuits. As expected, the circuit no. 4 with single amplifier (SAK) shows extremely high sensitivity (especially for higher pole-Q Chebyshev example) in the transient region near the pass-band edge frequency because it is the only 'medium-Q' circuit in the paper.

From Fig. 14, one can conclude that minimum noise possesses new LF filter as shown in Fig. 1 (curve no. 5 in Fig. 14), which can be used to process low-voltage signals submerged in noise. On the other hand, when needed for high-voltage signals this circuit can be modified into the circuit in Fig. 5, to be optimized for larger dynamic range, at the cost of larger noise floor (curve no. 6 in Fig. 14).

The poorest noise properties show no. 3 GIC and no. 4. SAK circuits. To conclude, *regarding the minimum noise and low sensitivity to component tolerances excellent performance in this paper possess the new LF filter shown in Fig. 1, which can be optimized for maximum dynamic range when needed.*

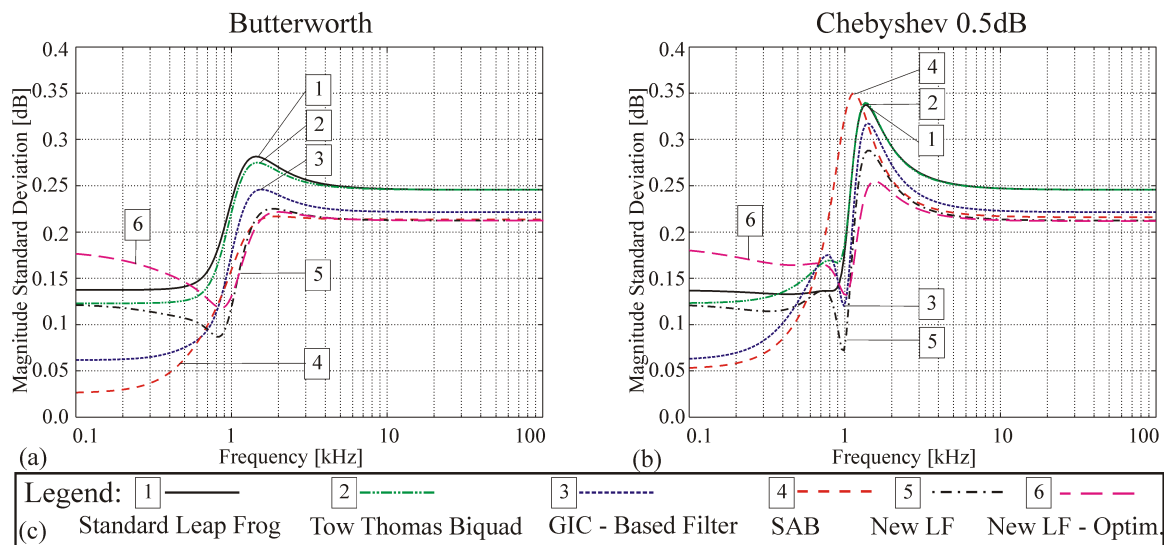


Fig. 13. Schoeffler sensitivities of classical filter blocks in this section, new LF filter, and new LF with optimized dynamic range (Matlab simulation). (a) Butterworth. (b) Chebyshev 0.5dB. (c) Legend

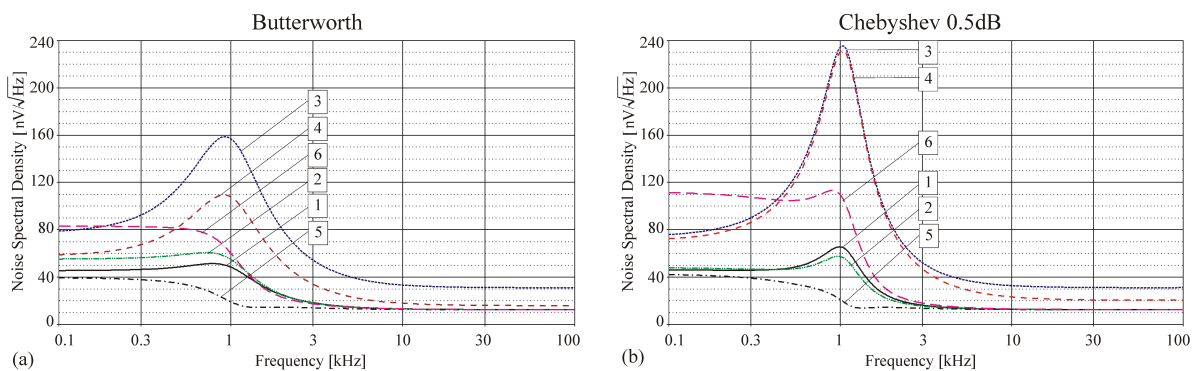


Fig. 14. PSpice output noise spectral density of classical filter blocks in this section, new LF filter, and new LF with optimized dynamic range (legend is in Fig. 13). (a) Butterworth. (b) Chebyshev 0.5dB

4 MEASUREMENT RESULTS

Measurements were performed on a Butterworth and a Chebyshev examples of 'new LF' filters (in Fig. 1), realized on separate printed circuit boards. Discrete 1% accurate resistors (E96 series) and 10% accurate capacitors (E12 series) were used together with the TL 081 A CPG4 Texas Instruments JFET input opamp (3MHz GBW product).

The two 'new LF filters' for Butterworth and Chebyshev 0.5dB examples were realized as discrete-component active-RC LP filters with a 1kHz cut-off frequency with components given in Table 2. For each filter, the output noise spectral density and amplitude-frequency characteristics (Bode diagrams) were measured using a typical university lab environment. The measurement equipment consisted of a high-quality HP 4195A Network Ana-

lyzer, which measures the spectrum of signals and/or noise (Spectrum mode), and Bode diagram (Network mode). Detailed description of measurement procedure and equipment is given in [16].

The measured amplitude-frequency characteristics are shown in Fig. 15. Observing Fig. 15 (and zoomed curves in the vicinity of cut-off frequency that are in the inset) one can conclude about *low sensitivity of 'new LF' filter* which provides accurate magnitude curves in spite of high tolerances of passive components.

The measured output-noise spectral-density runs of 'new LF' LP filters are presented in Fig. 16. Comparing the measured results in Fig. 16 with the results obtained from the PSpice simulation shown in Fig. 14 (curve 5) shows very good agreement between the two. *This reconfirms the low-noise performance of the 'new LF' filter.*

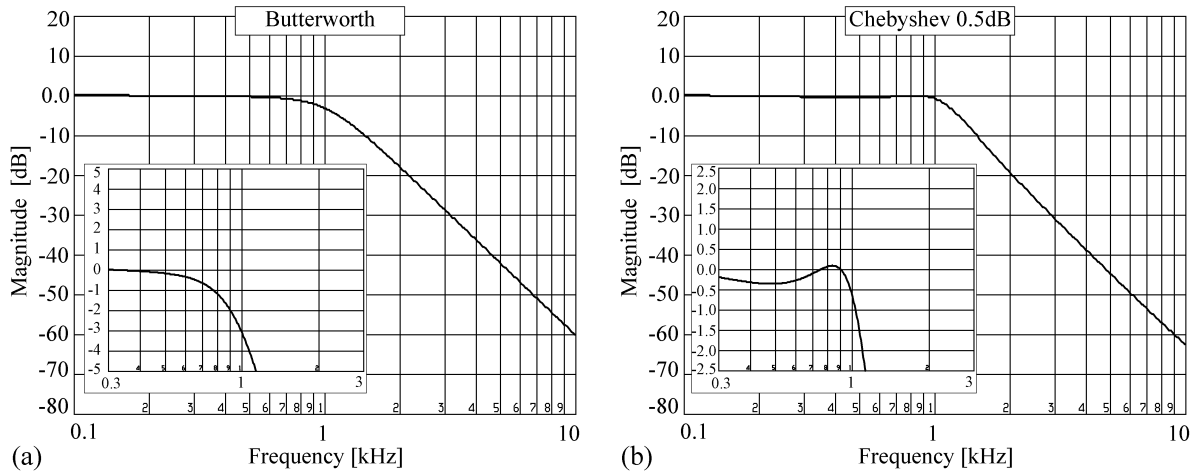


Fig. 15. Measured magnitude response of 'new LF' third-order low-pass filters (as in Fig. 1) having components given in Table 2. (a) Butterworth. (b) Chebyshev 0.5dB

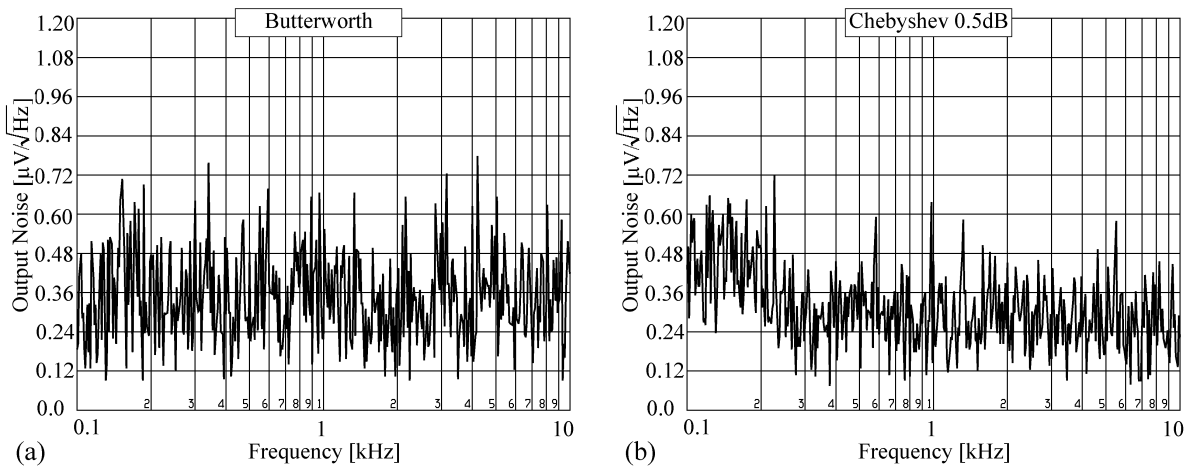


Fig. 16. Measured output noise spectral density of 'new LF' third-order low-pass filters (as in Fig. 1) having components given in Table 2. (a) Butterworth. (b) Chebyshev 0.5dB

Note that at higher frequencies only the thermal (Johnson) noise is apparent, i.e. the $1/f$ noise is too low to appear in the measurements.

5 CONCLUSION

The design procedures, as well as sensitivity and thermal output noise analyses were given for eight filter circuits that are suitable for realization of the third-order transfer function. The best performance showed the circuit denoted as new LF, which is proposed in this paper. Besides its design procedure, dynamic range numerical optimization was also presented on the modified new LF filter, which can be optimized for large signals without distortion.

ACKNOWLEDGMENT

This work has been financially supported by The National Foundation for Science, Higher Educations and Technological Development of the Republic of Croatia.

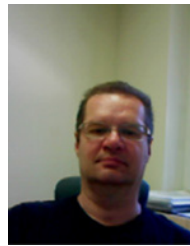
REFERENCES

- [1] D. Jurisic, G. S. Moschytz, and N. Mijat, "Low-sensitivity, single-amplifier, active-rc allpole filters using tables," *Automatika*, vol. 49, no. 3-4, pp. 159-173, 2008.
- [2] D. Jurisic, G. S. Moschytz, and N. Mijat, "Low-sensitivity active-rc allpole filters using optimized biquads," *Automatika*, vol. 51, no. 1, pp. 55-70, 2010.
- [3] M. Biey and A. Premoli, "Design of low-pass maximally flat rc-active filters with multiple real pole: The murromaf polynomials," *IEEE Transactions on Circuits and Systems*, vol. 25, no. 4, pp. 196-200, 1978.

- [4] N. Mijat, D. Jurisic, and M. Ranilovic, "Novel low-sensitivity, third-order lp active leap-frog filter," in *Proceedings of the 33rd MIPRO 2010*, (Opatija, Croatia), pp. 161–164, May 2010.
- [5] G. S. Moschytz and P. Horn, *Active Filter Design Handbook*. Chichester, UK.: John Wiley and Sons, 1981.
- [6] D. Jurisic, "Low-noise, low-sensitivity active-rc allpole filters using matlab optimization," in *Applications of MATLAB in Science and Engineering*, (Tadeusz Michalowski (Ed.)), pp. 197–224, InTech Publishers 2011.
- [7] *PSpice Users Guide ver. 16.5*. San Jose, CA-USA.: Cadence Design Systems, Inc. (Cadence), 2011.
- [8] *MATLAB: Optimization Toolbox*. Natick, MA-USA.: MathWorks, Inc., 2010.
- [9] D. Jurisic, N. Mijat, and G. S. Moschytz, "Dynamic range improvement of new leap-frog filter using numerical optimization," in *Proceedings of the 19th ICECS 2012*, (Seville, Spain), pp. 264–267, December 2012.
- [10] D. J. Perry, "Scaling transformation of multiple-feedback filters," *IEE Proceedings G Electronic Circuits and Systems*, vol. 128, no. 4, pp. 176–179, 1981.
- [11] R. Fletcher, *Practical Methods of Optimization*. Chichester, UK.: John Wiley and Sons, Volume 1, 1980.
- [12] N. Stojkovic, D. Jurisic, and N. Mijat, "Gic based third-order active low-pass filters," in *Proceedings of the 2nd ISPA 2001*, (Pula, Croatia), pp. 486–490, June 2001.
- [13] H. J. Orchard, "Inductorless filters," *Electronics Letters*, vol. 2, no. 6, pp. 224–225, 1966.
- [14] A. I. Zverev, *Handbook of Filter Synthesis*. New York, USA: John Wiley and Sons, 1967.
- [15] *Filter Designer 6.2*. Irvine, CA-USA.: Microsim Corporation, 1997.
- [16] D. Jurisic, N. Mijat, and M. Ranilovic, "Power consumption, noise and bode diagram measurement of active filters," in *Proceedings of the 34rd MIPRO 2011*, (Opatija, Croatia), pp. 92–95, May 2011.



Neven Mijat received his B.Sc., M.Sc. and Ph.D. degrees in Electrical Engineering from the Faculty of Electrical Engineering, University of Zagreb in 1970, 1974 and 1984, respectively. In 1970 he joined the Department of Electronic Systems and Information Processing at the Faculty of Electrical Engineering, University of Zagreb, where he is currently professor within the Networks, Systems and Signals group. At the Faculty he is involved in teaching lectures in undergraduate courses involving Network Theory, Filters, Analogue circuits, SC circuits, and in the postgraduate courses 'Filter design', and 'Numerical methods in system design'. His current research interests include data acquisition systems and filter theory and realization methods. He was also leading a number of R&D projects. He is member of IEEE, CROMBES, KoREMA and some other professional societies. He was a principal investigator for few scientific projects and development projects for companies. He received the 'Josip Loncar' silver plaques for his M.Sc. and Ph.D. theses in 1974 and 1984 respectively.



Dražen Jurišić is associate professor of the Faculty of Electrical Engineering at the University of Zagreb in Croatia where he received his B.Sc., M.Sc. and Ph.D. degrees in Electrical Engineering in 1990, 1995 and 2002, respectively. In 2005 he was elected as assistant professor and in 2011 as associate professor. He is involved in teaching lectures in undergraduate course on 'Electrical circuits', and in graduate course on 'Analog and mixed signal processing'. Present interests include analog and digital signal processing and filter design. From 1997 until 1999 he was with Swiss Federal Institute of Technology (ETH) Zürich, Switzerland, as holder of Swiss Federal Scholarship for Foreign Students doing Ph.D. research in the field of analog active-RC filters. He was rewarded with the silver plaque 'Josip Loncar' for his Ph.D. thesis. Since November 2008 he is visiting Bar-Ilan University, Israel and till now he spent 12 months there as a researcher. He is a member of KoREMA and IEEE-CAS society. He speaks English and German.



George S. Moschytz is Dean of the Faculty of Engineering at the Bar-Ilan University in Israel. Present interests include analog and digital, sampled-data, and adaptive filters, for communication systems. Earlier Professor Moschytz was with RCA Labs in Zürich, Bell Telephone Labs, Holmdel, NJ, where he supervised a group designing analog and digital integrated circuits for data communications, and at ETH, Zürich, as Professor and Director of the Institute for Signal and Information Processing. Author of 'Linear Integrated Networks: Fundamentals' and 'Linear Integrated Networks: Design', and co-author of the 'Active Filter Design Handbook', and 'Adaptive Filter' (in German). Editor of 'MOS Switched-Capacitor Filters: Analysis and Design', and co-editor of 'Tradeoffs in Analog Design'. Authored many papers in the field of network theory, design, and analysis, and holds numerous patents in these areas. Professor Moschytz has held the position of president of the IEEE Circuit and Systems Society, and is an elected member of the Swiss Academy of Engineering Sciences. He is a Life-Fellow of the IEEE, and has received several IEEE awards, including the IEEE CAS Education Award.

AUTHORS' ADDRESSES

Prof. Neven Mijat, Ph.D.

Associate Prof. Dražen Jurišić, Ph.D.

Department of Electronic Systems and Information Processing,

Faculty of Electrical Engineering and Computing, University of Zagreb,

Unska 3, HR-10000, Zagreb, Croatia

email: neven.mijat@fer.hr, drazen.jurisic@fer.hr

Prof. George S. Moschytz, Ph.D.

Faculty of Engineering,

Bar-Ilan University,

Ramat-Gan, IL-52900, Israel

email: George-S.Moschytz@biu.ac.il

Received: 2012-06-29

Accepted: 2012-07-21